

PAPER • OPEN ACCESS

Series solutions of \mathcal{PT} -symmetric Schrödinger equations

To cite this article: Carl M Bender *et al* 2018 *J. Phys. Commun.* **2** 025012

Recent citations

- [Quantum dynamics of a parity-time-symmetric kicked particle in a 1D box](#)
J Yusupov *et al*
- [PT-symmetric quantum graphs](#)
D U Matrasulov *et al*

View the [article online](#) for updates and enhancements.



PAPER

OPEN ACCESS

RECEIVED
20 November 2017REVISED
2 January 2018ACCEPTED FOR PUBLICATION
19 January 2018PUBLISHED
7 February 2018

Original content from this work may be used under the terms of the [Creative Commons Attribution 3.0 licence](#).

Any further distribution of this work must maintain attribution to the author(s) and the title of the work, journal citation and DOI.

Series solutions of \mathcal{PT} -symmetric Schrödinger equationsCarl M Bender¹ , C Ford² , Nima Hassanpour¹ and B Xia²¹ Department of Physics, Washington University, St. Louis, Missouri 63130, United States of America² Department of Mathematics, Imperial College London, London SW7 2AZ, United KingdomE-mail: cmb@wustl.edu, c.ford@imperial.ac.uk, nimahassanpourghahy@wustl.edu and bichang.xia13@imperial.ac.uk**Keywords:** PT symmetry, numerical calculation of eigenvalues, eigenfunctions, matrix elements

Abstract

A simple and accurate numerical technique for finding eigenvalues, node structure, and expectation values of \mathcal{PT} -symmetric potentials is devised. The approach involves expanding the solution to the Schrödinger equation in series involving powers of both the coordinate and the energy. The technique is designed to allow one to impose boundary conditions in \mathcal{PT} -symmetric pairs of Stokes sectors. The method is illustrated by using many examples of \mathcal{PT} -symmetric potentials in both the unbroken- and broken- \mathcal{PT} -symmetric regions.

1. Numerical procedure

The area of research known as \mathcal{PT} -symmetric quantum theory began with the discovery that the complex \mathcal{PT} -symmetric Schrödinger equation

$$-\psi''(z) - (iz)^N \psi(z) = E\psi(z) \quad (1)$$

has real spectra if $N \geq 2$ [1–3]. This is called the region of *unbroken* \mathcal{PT} symmetry. If $0 < N < 2$ the spectrum is partly real and partly complex; this is called the region of *broken* \mathcal{PT} symmetry. Since this early work, research on \mathcal{PT} -symmetric systems has spread to many other areas of physics such as optics [4–6] and nonlinear wave equations [7, 8] to mention just a few.

If N is integer, the eigenfunctions are entire functions and the complex plane splits naturally into $N + 2$ Stokes wedges. (For the numerical technique described in this paper N need not be an integer, as we will see in section 3). Energy quantization is a consequence of demanding that $\psi(z)$ decay exponentially in a \mathcal{PT} -symmetric pair of Stokes sectors. For any energy E , real or complex, there is a solution that decays exponentially in any given wedge. For special values of E one can find solutions that decay in two (noncontiguous) wedges. (Note that we are using the notation $-(iz)^N$ that was used in [1] to represent \mathcal{PT} -symmetric potentials. Subsequently, the notation $x^2(ix)^\varepsilon$ was used. However, the original notation is more suitable for the series techniques described in this paper.)

In [9] a technique for finding the eigenvalues of a Schrödinger equation (1) was explored that involved expanding the eigenfunctions as formal perturbation series in powers of the energy E . The technique was moderately effective, although it sometimes required the use of summation techniques to handle divergent series. In this paper we extend this technique to include series in powers of *both* iz and E . Consider the double power series

$$\psi_1(z) = \sum_{p=0}^{\infty} \sum_{q=0}^{\infty} a_{p,q} (iz)^{(N+2)p+2q} E^q, \quad (2)$$

where the $a_{p,q}$ are constants. Because the parameter N appears in the power of iz , if we insert this series into the Schrödinger equation (1), we obtain a particularly simple recursion relation for the coefficients $a_{p,q}$:

$$[(N+2)p+2q-1][(N+2)p+2q]a_{p,q} = a_{p-1,q} + a_{p,q-1}. \quad (3)$$

Viewing $a_{p,q}$ as a matrix, (3) expresses the element $a_{p,q}$ in terms of the elements that are immediately adjacent. Thus, on fixing the top left element $a_{0,0}$ one can, in principle, determine all the other elements. For the

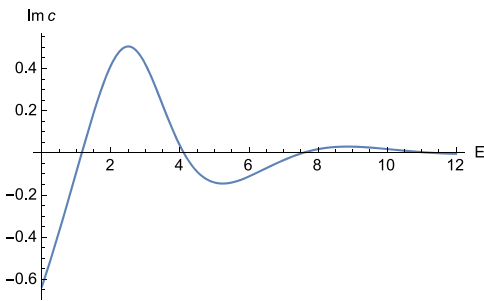


Figure 1. The value of $\text{Im } c$ plotted as a function of E . The first few energy levels in the $N = 3$ theory appear as roots of $\text{Im } c$.

convenient choice $a_{0,0} = 1$ all the $a_{p,q}$ are positive rational numbers. (This is because the \mathcal{PT} symmetry of the series representation is enforced by this structure). With this choice $\psi_1(0) = 1$ and $\psi_1'(0) = 0$.

A second solution of the Schrödinger equation is

$$\psi_2(z) = \sum_{p=0}^{\infty} \sum_{q=0}^{\infty} b_{p,q} (iz)^{1+(N+2)p+2q} E^q, \quad (4)$$

where the coefficients $b_{p,q}$ satisfy the recursion relation

$$[(N+2)p+2q][(N+2)p+2q+1]b_{p,q} = b_{p-1,q} + b_{p,q-1}. \quad (5)$$

It is convenient to take $b_{0,0} = 1$ so that $\psi_2(0) = 0$ and $\psi_2'(0) = i$.

Now consider a linear combination of the two solutions

$$\psi(z) = \psi_1(z) + c\psi_2(z),$$

where c is a complex constant. By a suitable choice of c one can ensure that $\psi(z)$ decays exponentially in any one of the $N + 2$ Stokes sectors. For example, to obtain decay in the sector centered at (the anti-Stokes line) $\theta = -\frac{1}{2}\pi(N-2)/(N+2)$ take

$$c = -\lim_{r \rightarrow \infty} \frac{\psi_1(re^{i\theta})}{\psi_2(re^{i\theta})} \Big|_{\theta = -\frac{1}{2}\pi(N-2)/(N+2)}. \quad (6)$$

This works for any E but it only gives a decaying wave function in one of the $N + 2$ sectors. However, the key point of this paper is that *if both E and c are real, then the solution will also decay in the \mathcal{PT} image of the sector*. This is the crucial step in the numerical procedure because it makes explicit use of the \mathcal{PT} symmetry of the potential.

To determine the spectrum associated with a \mathcal{PT} symmetric pair of sectors it suffices to determine the real energies for which c is real. This can be implemented graphically by plotting $\text{Im } c$ as a function of E . The zeros of this plot correspond to the energy levels. In figure 1 $\text{Im } c$ is plotted for $N = 3$. Note that as E increases, $\text{Im } c$ approaches zero in an oscillatory fashion. $\text{Im } c$ has no roots for negative E . To produce this plot we made two approximations:

- (i) In the double power series (2) and (4) we retained all terms with $p + q \leq 100$.
- (ii) In (6) a large finite value of r (in this case $r = 8$) was taken instead of the $r \rightarrow \infty$ limit.

In matrix language the truncation is *anti-diagonal* in the sense that entries below the $p + q = 100$ line are discarded. By applying a root-finding algorithm to the approximation for $c(E)$ we can compute the energy levels and associated values of $\text{Re } c$. These are given in table 1.

For large values of n the value of c_n is approximately $-\sqrt{E_n}$. To investigate the accuracy of the numerical scheme one can vary the $p + q \leq 100$ truncation and the r value. The numerical results for the first few energy levels are not affected by taking $r = 7$ instead of $r = 8$ at least to 20 significant figures. Similarly, increasing the truncation to $p + q \leq 150$ does not change the first few energy levels (again to 20 significant figures). However, the higher energy levels are more sensitive to changes in r and to the truncation. We have quoted E_4 to 17 rather than 20 significant figures as the missing three digits change when the truncation is improved. For higher n the accuracy drops further. As the double power series are expansions in iz and E , we expect that the truncation is less accurate for higher energies. Our energy levels are consistent with the Runge-Kutta based results reported in [10].

For higher N there is more than one pair of (nonadjacent) \mathcal{PT} -symmetric sectors [11]. Indeed, if N is odd, there are $\frac{1}{2}(N-1)$ such pairs. If N is even, there are $\frac{1}{2}(N+2)$ pairs; one of these pairs is both \mathcal{PT} symmetric

Table 1. Energy levels and c values in the $N = 3$ theory.

n	E_n	c_n
0	1.1562670719881132937	-0.53871550451988192490
1	4.1092287528096515358	-2.32727424075874334001
2	7.5622738549788280413	-2.69833514190279036708
3	11.314421820195804397	-3.37823419494258452822
4	15.291553750392532	-3.90980926012776641
5	19.451529130691	-4.41178037226863
6	23.766740435	-4.87570168194
7	28.2175249	-5.312499663

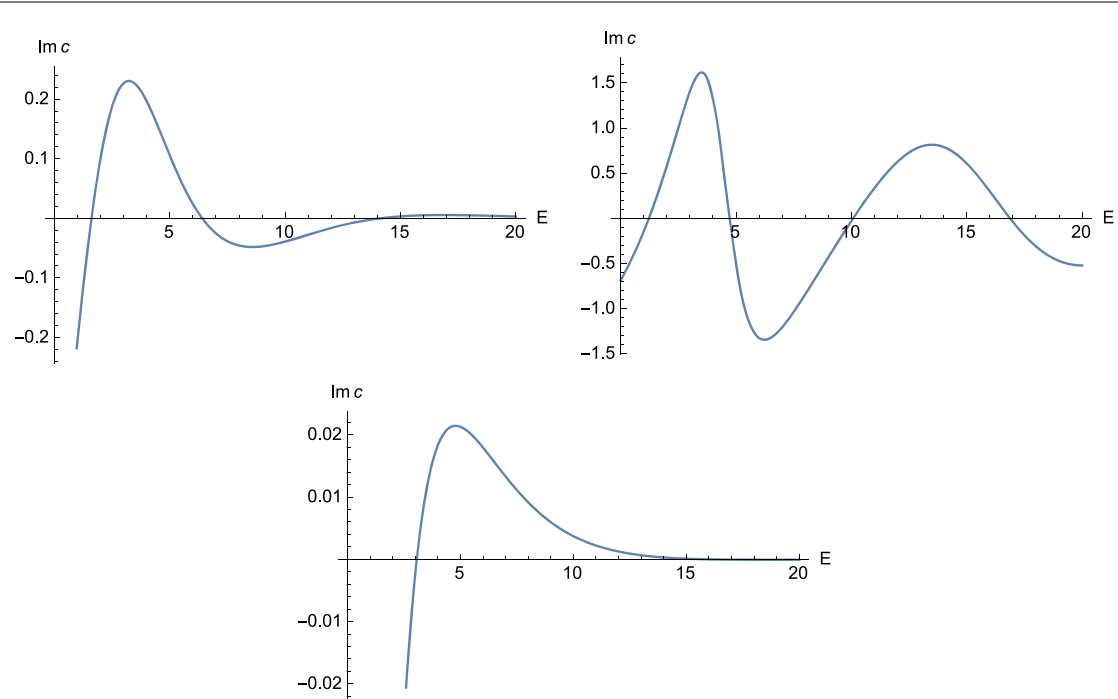


Figure 2. $\text{Im } c$ in the $N = 7$ theory for three \mathcal{PT} -symmetric spectra. The upper left plot is for the wedges centered at $\theta = \pi/6$ and $\theta = 5\pi/6$; the upper right plot has wedges centered at $\theta = -\pi/18$ and $\theta = -17\pi/18$; the lower plot has wedges centered at $\theta = -5\pi/18$ and $\theta = -13\pi/18$.

and \mathcal{P} symmetric. The graphical method used here is also applicable in this case but the energy eigenstates are of the form ψ_1 (even parity) or ψ_2 (odd parity). In this case one may have to interchange the roles of ψ_1 and ψ_2 in (6) to obtain all the eigenvalues. (This is discussed in section 3).

To illustrate what happens for large values of N we examine the case $N = 7$. There are three \mathcal{PT} -symmetric pairs if $N = 7$. Each pair gives a distinct real and positive spectrum; $\text{Im } c$ is plotted in figure 2 as a function of E for the three pairs.

For higher n the E_n have ratios 1.41:1:3.52 [11]. Although our method is adapted to small n , such behavior is evident in the third excited state; E_3 has values 23.702, 16.872, 59.026. The ratios of the energies are different; E_0 has values 1.6047, 1.2247, 3.0686.

For the upper spectrum (that is, with wedges centered at $\theta = \pi/6$ and $\theta = 5\pi/6$) the c_n values are positive with $c_n \approx \sqrt{E_n}$ for large n . The other two spectra yield negative c_n with $c_n \approx -\sqrt{E_n}$. The plots were produced via the same $p + q \leq 100$ truncation but with $r = 3$ rather than $r = 8$ ³. Similar results can be obtained for higher N . For example, the $N = 19$ model has 9 distinct spectra (4 giving positive c_n , 5 with negative c_n).

2. Nodes and expectation values

The truncations considered here can be used to identify the nodes and expectation values of the energy eigenstates. Although our truncation is inaccurate for large enough $|z|$, at least for the first few energy levels the

³ For $N = 7$ the truncation breaks down for lower $|z|$.

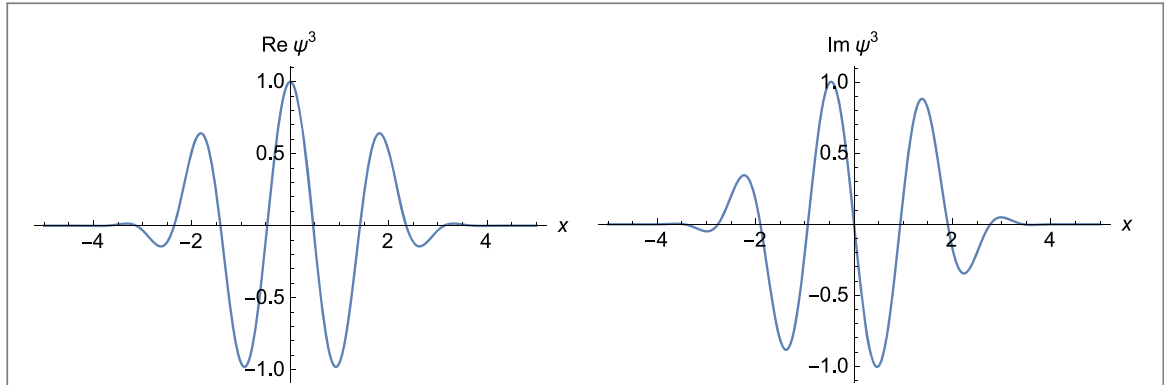


Figure 3. Eigenfunction for the third excited state for $N = 3$ plotted along the real axis.

Table 2. Expectation values $\langle z^m \rangle_n$ in the $N = 3$ theory.

n	0	1	2	3
m				
1	-0.5900725330i	-0.9820718380i	-1.2054807539i	-1.3796870779i
2	0	0	0	0
3	-0.4625068288i	-1.6436915011i	-3.0249095421i	-4.5257687286i
4	-0.3898751086	-2.3060330480	-5.2092431933	-8.9202066199

nodes are close enough to the origin for them to be determined with high precision. Returning to the $N = 3$ case, we note that all energy eigenfunctions have an infinite string of zeros on the positive imaginary axis; for each energy level these lie above the classical turning point at $iE_n^{1/3}$. In addition, the n th excited state has n nodes below the real axis (the first excited state has a node at $z = -0.661296226442715413308i$). The n nodes arch above and between the classical turning points at $E_n^{1/3}e^{-i\pi/6}$ and $E_n^{1/3}e^{-5\pi/6}$ [12].

An interesting question considered in [13] is the precise form of the arch for large n . Unlike the $N = 2$ harmonic oscillator the nodes do not lie on the classical trajectory joining two turning points. In fact, for $N = 3$ this trajectory is exactly circular with its center at the turning point on the imaginary axis [14].

The approximation method introduced here may be used to compute expectation values. If $\psi(z)$ is an energy eigenstate, then the expectation value of z^m is a ratio of contour integrals⁴:

$$\langle z^m \rangle = \frac{\int_C dz \psi(z) z^m \psi(z)}{\int_C dz \psi(z) \psi(z)},$$

where C is any curve that divides the complex plane in two and starts in one wedge and ends in the \mathcal{PT} -symmetric wedge. For $N = 3$ one can simply choose C to be the real line:

$$\langle z^m \rangle_n = \frac{\int_{-\infty}^{\infty} dx \psi^n(x) x^m \psi^n(x)}{\int_{-\infty}^{\infty} dx \psi^n(x) \psi^n(x)},$$

where ψ^n is the n th energy eigenstate ($n = 0, 1, 2, 3, \dots$). As the wave functions decay exponentially these integrals over the real line are well approximated by integrals over a finite range $[-\lambda, \lambda]$ for sufficiently large λ . We have computed expectation values for the first few energy eigenstates in the $N = 3$ model. We have cut off the integrals at $\lambda = 5$ and have approximated the ψ_1 and ψ_2 with the truncation ($p + q \leq 100$) described above. Plots of the wave functions indicate that the cut off $\lambda = 5$ is a good approximation for the first few eigenstates; a plot of $\psi^3(x)$ is given in figure 3 and the expectation values $\langle z^m \rangle_n$ in the $N = 3$ are listed in table 2.

In our approximation $\langle z^2 \rangle_m$ is small ($\langle z^2 \rangle_0 \approx 10^{-11}$). This is because $\langle z^2 \rangle_n$ is exactly zero. To see why this is true, we note that $I = \int_{-\infty}^{\infty} dx x^2 \psi^2(x) = \frac{1}{3} \int_{-\infty}^{\infty} dx (x^3) \psi^2(x)$. Upon integrating by parts, we get

$I = -\frac{2}{3} \int_{-\infty}^{\infty} dx x^3 \psi(x) \psi'(x)$. Finally, we use the Schrödinger equation (1) with $N = 3$ to replace $x^3 \psi(x)$ with a linear combination of $\psi''(x)$ and $\psi(x)$ and observe that each term is an exact derivative that integrates to zero.

⁴ Note that if ψ is not an energy eigenstate, this formula is not valid. Expectation values must then be computed via a modified inner product in terms of a new operator \mathcal{C} [15]. This inner product is related to the standard Dirac inner product via a nonunitary similarity transformation [16].

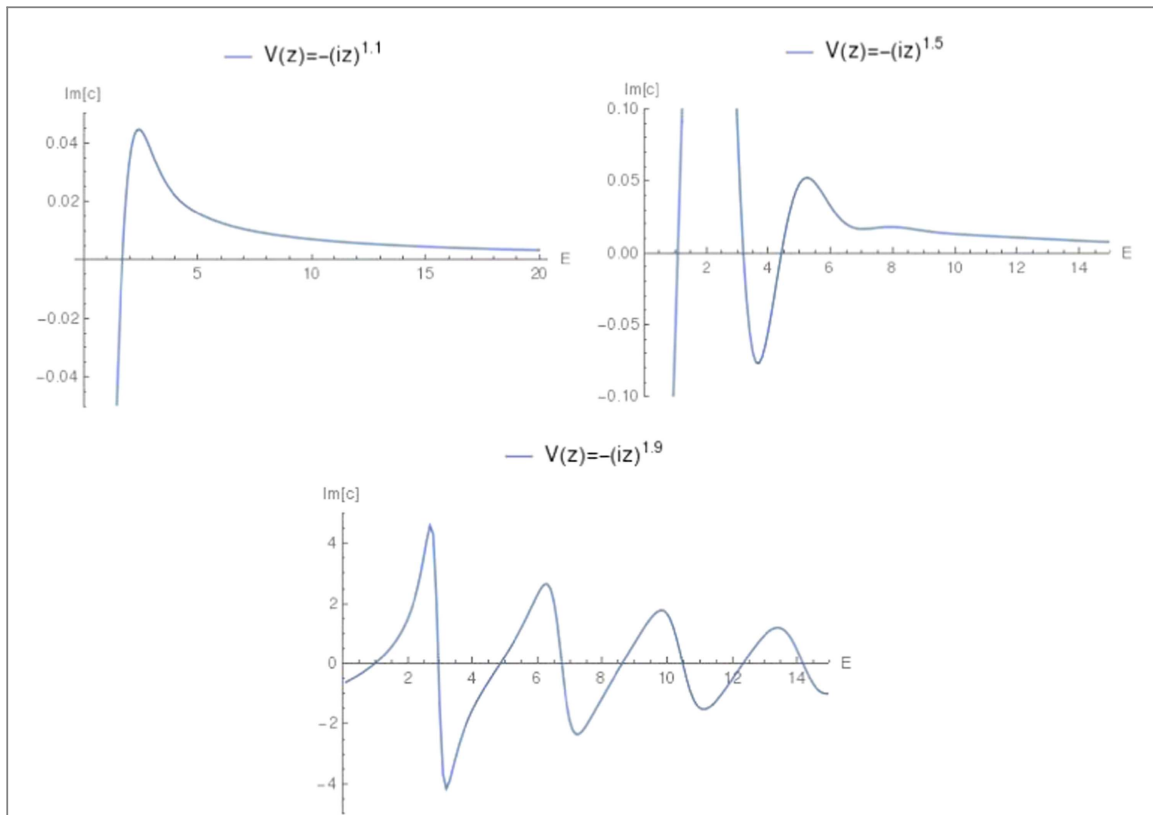


Figure 4. Plot of $\text{Im}[c]$ for the $N = 1.1$, $N = 1.5$, and $N = 1.9$ theories. All three of these theories are in the \mathcal{PT} broken region. In the first case there is only one real eigenvalue, in the second case there are three real eigenvalues, and in the third case there are many real eigenvalues. In all cases the numerical method used here provides highly accurate results.

Table 3. Eigenvalues in the broken \mathcal{PT} regime for noninteger values of N .

$N = 1.1$		$N = 1.5$		$N = 1.9$	
n	Series soln	n	Series soln	n	Series soln
0	1.6836723247	0	1.08692903345877	0	1.0015867791272
1	—	1	3.195783621829	1	2.957492901530
2	—	2	4.42201575335	2	4.85886246929
3	—	3	—	3	6.7482128957
4	—	4	—	4	8.6180610339

For general N similar calculations indicate that $\langle z^{N-1} \rangle_n$ is zero for all \mathcal{PT} -symmetric pairs of Stokes wedges. This is a \mathcal{PT} -symmetric example of the Ehrenfest theorem. One can also see a \mathcal{PT} -symmetric virial theorem in the $N = 3$ expectation values; $\langle z^3 \rangle_n$ is exactly $-\frac{2}{5}iE_n$. This can be written as $\langle V \rangle_n = \frac{2}{5}E_n$.

3. Numerical scheme applied to other potentials

The numerical scheme described in section 1 does not require that N be an integer. Therefore, we can consider noninteger values of N in both the broken and unbroken \mathcal{PT} -symmetric regions. We first study three values of N in the \mathcal{PT} broken region: $N = 1.1, 1.5, 1.9$. As one can see in [1] there is only one real eigenvalue for $N = 1.1$, three real eigenvalues for $N = 1.5$, and many real eigenvalues for $N = 1.9$ as indicated by the results in figure 4 and table 3.

Next we examine two values of N in the \mathcal{PT} unbroken region: $N = 2.1$ and $N = 2.5$. In this case there are an infinite number of real eigenvalues and no complex eigenvalues. Once again, our numerical procedure gives highly accurate results for these cases. See figure 5 and table 4.

A particularly interesting \mathcal{PT} -symmetric potential is $V = -(iz)^4$. While this may naively appear to be an upside down potential, when we quantize the theory by imposing boundary conditions in a pair of Stokes sectors in the complex plane, we find that the spectrum is entirely real and positive. (An elementary proof of this is given in [17]). Moreover, the spectrum of this potential is different from that of the quartic anharmonic oscillator

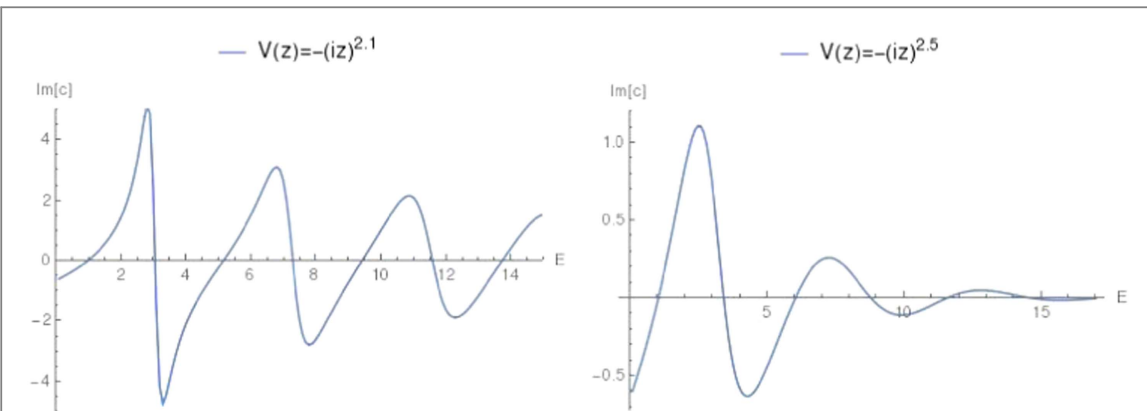


Figure 5. Plot of $\text{Im } c$ for the $N = 2.1$ and $N = 2.5$ theories. These two theories are in the \mathcal{PT} unbroken region. In the first case there is only one real eigenvalue, in the second case there are three real eigenvalues, and in the third case there are many real eigenvalues. In all cases the numerical method used here provides highly accurate results.

Table 4. Eigenvalues in the unbroken \mathcal{PT} regime for noninteger values of N .

$N = 2.1$		$N = 2.5$	
n	Series soln	n	Series soln
0	1.003097514661	0	1.048954090261
1	3.06113230366	1	3.43453593249
2	5.16708540045	2	6.05173796085
3	7.2921244575	3	8.7910138373
4	9.4332388593	4	11.6206954696

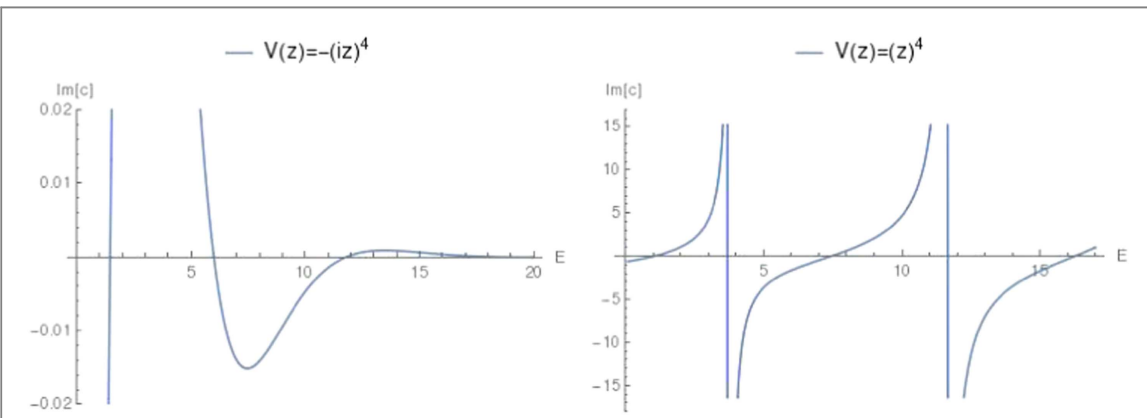


Figure 6. Plot of $\text{Im } c$ for the potentials $V = -x^4$ and $V = x^4$.

($V = x^4$). We can easily apply the numerical techniques described in this paper to find the eigenvalues of both of these potentials because both potentials are real functions of iz (see figure 6).

The eigenvalues for the potentials $V = -x^4$ and $V = x^4$ and also those of the harmonic oscillator $V = x^2$ are listed below in table 5. As we can see in figure 6, for potentials that are parity symmetric, such as x^4 , the slope of the curve typically alternates between being very steep and not very steep when it crosses the horizontal axis. When the slope is steep it is numerically more difficult for the computer software to determine the precise value of E . This explains the varying accuracy in the eigenvalues for the x^2 potential, for example. To improve numerical accuracy one can do two things. First, one can compute the curve using a finer mesh of grid points. Second, one can interchange the roles of ψ_1 and ψ_2 in (6) to make the curve less steep.

Finally, we emphasize that our numerical technique is not limited to monomial potentials. It applies equally well to multinomial potentials $V(z)$ that are \mathcal{PT} symmetric; that is, potentials that are real functions of iz . Thus, for the Schrödinger equation (1) in which the potential has the form

Table 5. Eigenvalues of the harmonic oscillator $V = x^2$ ($N = 2$), the \mathcal{PT} -symmetric quartic oscillator $V = -x^4$ ($N = 4$), and the conventional anharmonic oscillator $V = x^4$ obtained by using the numerical methods described in this paper.

$V = x^2$		$V = -x^4$		$V = x^4$	
n	Series soln	n	Series soln	n	Series soln
0	1.0000000000004	0	1.4771508111864	0	1.060363864841
1	2.999999999999993	1	6.0033861147867	1	3.799673009836
2	4.99999999997	2	11.8024336007832	2	7.45569799483
3	6.99999999997	3	18.458818772430	3	11.6447453215
4	9.000000001	4	25.79178997784	4	16.2618260301

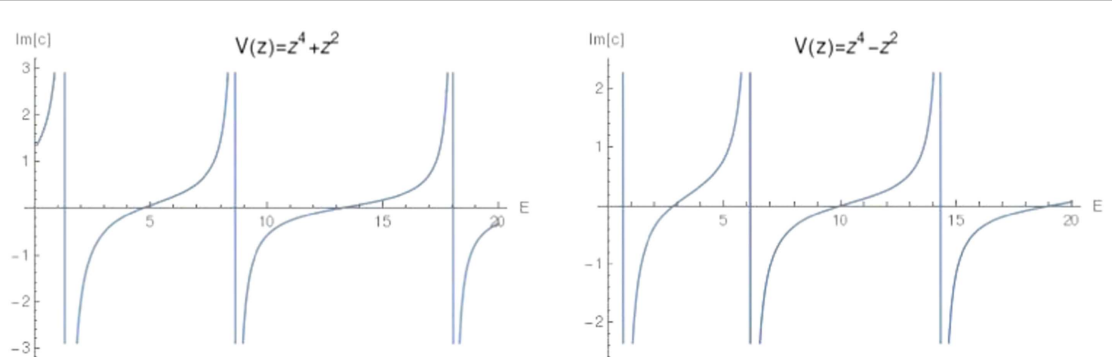


Figure 7. Plot of $\text{Im } c$ for the anharmonic oscillator potentials $V = x^4 \pm x^2$.

$$V(z) = c_1(iz)^N + c_2(iz)^M$$

we define the two solutions ψ_1 and ψ_2 as triple sums rather than double sums:

$$\psi_1(z) = \sum_{p=0}^{\infty} \sum_{r=0}^{\infty} \sum_{q=0}^{\infty} a_{p,q,r}(iz)^{(N+2)p+(M+2)r+2q} E^q$$

and

$$\psi_2(z) = \sum_{p=0}^{\infty} \sum_{r=0}^{\infty} \sum_{q=0}^{\infty} b_{p,q,r}(iz)^{1+(N+2)p+(M+2)r+2q} E^q.$$

These lead to the two recursion relations

$$[(N+2)p + (M+2)r + 2q][(N+2)p + (M+2)r + 2q - 1]a_{p,r,q} = -c_1a_{p-1,q,r} - c_2a_{p,r-1,q} + a_{p,r,q-1}$$

and

$$[(N+2)p + (M+2)r + 2q + 1][(N+2)p + (M+2)r + 2q]b_{p,r,q} = -c_1b_{p-1,q,r} - c_2b_{p,r-1,q} + b_{p,r,q-1},$$

which are the generalizations of (3) and (5).

If we apply these techniques to the massive quartic anharmonic oscillators with either positive or negative mass terms $V(x) = x^4 \pm x^2$, we again obtain excellent numerical results for the low-lying eigenvalues (see figure 7).

Indeed, table 6 shows the numerical scheme works equally well for the single-well and the double-well anharmonic oscillator.

However, if the potential is *not* a real function of the variable iz , then the numerical methods described here do not work. To illustrate this we consider the potential $V(x) = x^4 + x$. Table 7 shows that the eigenvalue calculation fails.

In conclusion, we have demonstrated in this paper an extremely powerful and highly accurate technique for computing the eigenvalues (and eigenfunctions) of a \mathcal{PT} -symmetric potential. We have established the accuracy of the method by studying a large number of examples. Our technique is important because it addresses the difficult problem of solving complex non-Hermitian eigenvalue problems. Most conventional techniques for solving real Hermitian eigenvalue problems fail to work for complex eigenvalue problems because complex eigenvalue problems must be solved subject to boundary conditions imposed in Stokes sectors in the complex plane. Of course, our technique also works very well for real eigenvalue problems, so long as the real potential is \mathcal{PT} symmetric.

Table 6. Eigenvalues of the single-well ($V = x^4 + x^2$) and double-well ($V = x^4 - x^2$) quartic anharmonic oscillators obtained by using the numerical methods described in this paper. The numerical accuracy is excellent and is roughly the same for either oscillator.

$V = x^4 + x^2$		$V = x^4 - x^2$	
n	Series soln	n	Series soln
0	1.39235191352537	0	0.657656758014
1	4.648811867490	1	2.834533175294
2	8.65505000457	2	6.16390133772
3	13.1568037536	3	10.0386458708
4	18.0575574491	4	14.372406513
5	23.2974414415	5	19.085714647

Table 7. This table shows that the numerical methods used in this paper fail if the potential is not \mathcal{PT} symmetric; that is, it is not a real function of the variable iz .

$V(x) = x^4 + x$		
n	Wrong!	Exact
0	0.991863	0.9305
1	1.53021	3.7819
2	8.42823	7.4351
3	17.4568	11.6283
4	27.8829	16.2478

ORCID iDs

Carl M Bender  <https://orcid.org/0000-0002-3840-1155>

References

- [1] Bender C M and Boettcher S 1998 *Phys. Rev. Lett.* **80** 5243
- [2] Bender C M, Boettcher S and Meisinger P 1999 *J. Math. Phys.* **40** 2201
- [3] Dorey P, Dunning C and Tateo R 2001 *J. Phys. A* **34** 5679
- [4] Guo A, Salamo G J, Duchesne D, Morandotti R, Volatier-Ravat M, Aimez V, Siviloglou G A and Christodoulides D N 2009 *Phys. Rev. Lett.* **103** 093902
- [5] Rüter C E, Makris K G, El-Ganainy R, Christodoulides D N, Segev M and Kip D 2010 *Nat. Phys.* **6** 192
- [6] Lin Z, Ramezani H, Eichelkraut T, Kottos T, Cao H and Christodoulides D N 2011 *Phys. Rev. Lett.* **106** 213901
- [7] Musslimani Z H, Makris K G, El-Ganainy R and Christodoulides D N 2008 *Phys. Rev. Lett.* **100** 030402
- [8] Dai C Q, Wang X G and Zhou G Q 2014 *Phys. Rev. A* **89** 013834
- [9] Bender C M and Jones H F 2014 *J. Phys. A: Math. Theor.* **47** 395303
- [10] Bender C M 2007 *Rept. Prog. Phys.* **70** 947
- [11] Schmidt S and Klevansky S P 2013 *Phil. Trans. Roy. Soc. Lond. A* **371** 20120049
- [12] Bender C M, Cooper F, Meisinger P and Savage V M 1999 *Phys. Lett. A* **259** 224
- [13] Bender C M, Boettcher S and Savage V M 2000 *J. Math. Phys.* **41** 6381
- [14] Jennings D 2011 *University of East Anglia Undergraduate Project Report* unpublished
- [15] Bender C M, Brod J, Refiq A and Reuter M 2004 *J. Phys. A* **37** 10139
- [16] Mostafazadeh A 2003 *J. Math. Phys.* **44** 974
- [17] Bender C M, Brody D C, Chen J-H, Jones H F, Milton K A and Ogilvie M C 2006 *Phys. Rev. D* **74** 025016